Electronic Supplementary Information

The effect of guanidinium functionalization on the structural properties and anion affinity of polyelectrolyte multilayers

Zheng Cao,‡[ab] Pavlo I. Gordiichuk,[c] Katja Loos,[c] Ernst J.R. Sudhölter,[a] Louis C.P.M. de Smet*[a]

[a] *Organic Materials and Interfaces, Department of Chemical Engineering, Delft University of Technology, Julianalaan 136, 2628 BL Delft, The Netherlands. Email: l.c.p.m.desmet@tudelft.nl*
[b] *Wetsus, centre of excellence for sustainable water technology, Oostergoweg 9, 8911 MA Leeuwarden, The Netherlands*
[c] *Zernike Institute for Advanced Materials, University of Groningen, Nijenborgh 4, 9747 AG Groningen, The Netherlands*
‡ Current address: School of Materials Science and Engineering, Changzhou University, China

Contents Electronic Supplementary Information

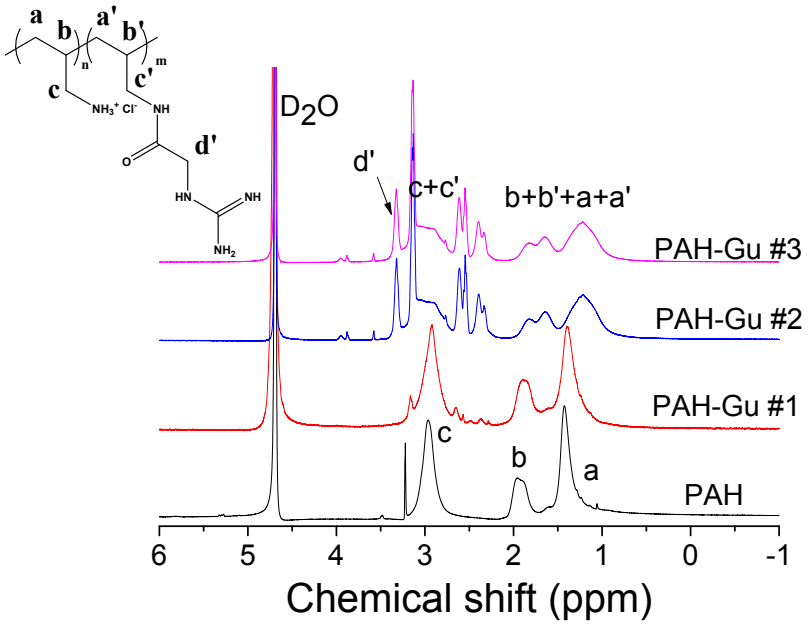

Fig. S1. ^{1}H NMR spectra of PAH and the series of synthesized PAH-Gu polymers. The ^{1}H NMR spectra were measured in D_2O using a Bruker AVANCE 400 NMR spectrometer.

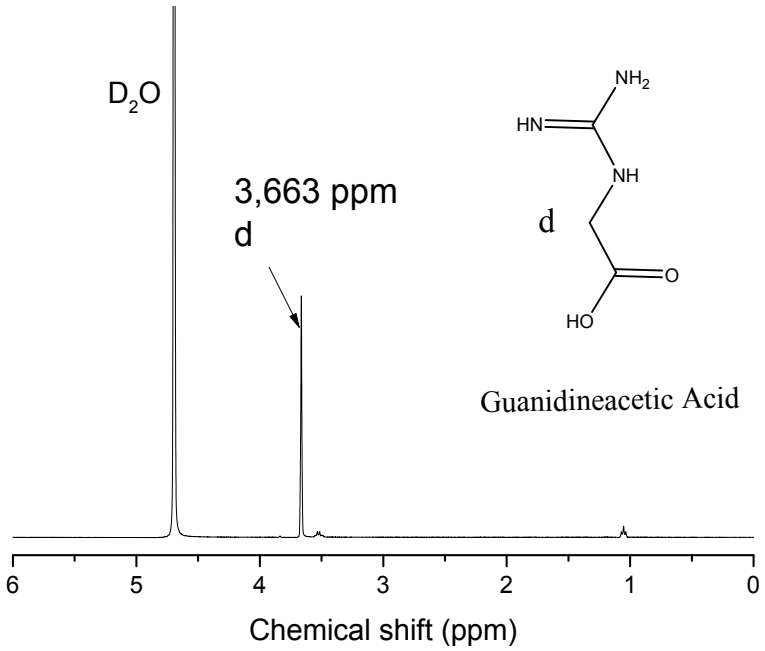

Fig. S2. ^{1}H NMR spectrum of guanidineacetic acid. Peak d originates from the CH_2 protons located close to the amino and hydroxyl groups characteristic of amino acids, which is in agreement with the result reported in SciFinder database. The ^{1}H NMR spectrum was measured in D_2O using a Bruker AVANCE 400 NMR spectrometer.

The integral intensities of the peaks (b, b', a, a') of -CH_2-CH- protons in the main chains at 0.8-2.1 ppm and the characteristic peak (d') of CH_2 protons in the side group were used to calculate the approximate content of the modified and unmodified allylamine units in the polymers (Fig. **S1**).

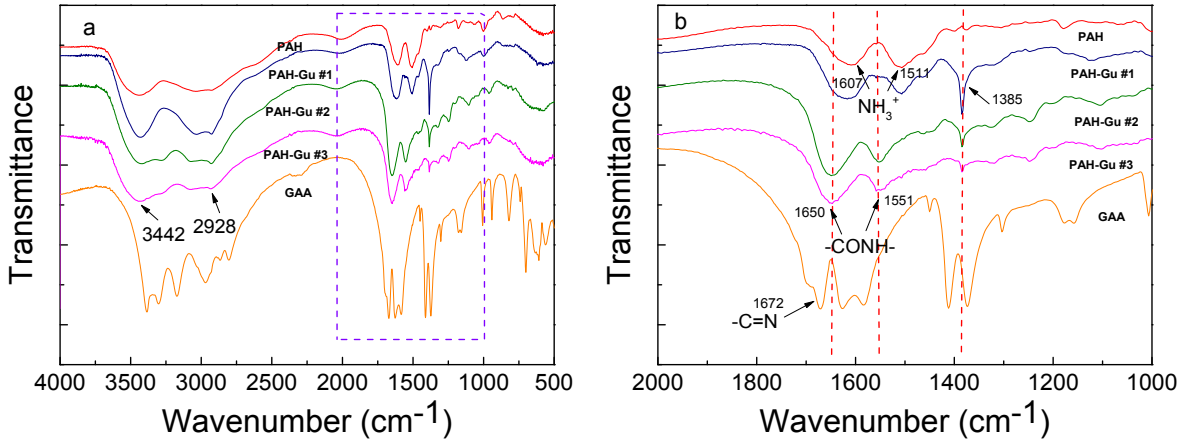

Fig. S3. FT-IR spectra of PAH, the PAG-Gu series (#1, #2 and #3) and guanidineacetic acid (GAA).

Table S1. Summary of the parameters calculated with the Voigt model using the QTools option 'Extended viscoelastic models for f and D' for the complex viscoelastic films (top entries), including reference data taken from literature (bottom entries).

System modelled with QTools	Layer density ($Kg \cdot m^{-3}$)	Layer viscosity (mPa·s)	Layer shear modulus (Pa)	Source
PSS/PAH PEM	1000	4.3	231060	Current work
PSS/PAH-Gu PEM	1000	10.8	147520	Current work
PEM of chitosan & alginate	1400	12	60000	Ref 1
Protein film (M_w 120 kDa)	Prior to crosslinking: 1040; after crosslinking: 1180	Prior to crosslinking: 1.8; after crosslinking: 6	Prior to crosslinking: 66000; after crosslinking: 300000	Ref 2
PAH/PAA PEM	1200	~10	~600000	Ref 3

The thickness of the PEMs was obtained by fitting the data with the Voigt model, where the PEM density, the fluid density and the viscosity are taken to be 1000 kg m^{-3}, 1000 kg m^{-3} and 1 m Pa s, respectively. In QTools the option "Extended viscoelastic models for f and D" was selected for the modelling. After modelling, it was found that the fitted and measured curves overlapped well, indicating a good fit by using the Voigt model. It is noted that the QTools options 'Viscoelastic models for f and D' and 'Extended viscoelastic models for f and D' gave the same results. Comparison with literature data (Table S1) learns that the values obtained in the current study are within the proper range.

Table S2. Summary of the water content calculations based on the optical and wet thickness and the corresponding frequency shift of the PAH-Gu/QCM sensors after being exposed to the different anion solutions.

	Cl^-	NO_3^-	SO_4^{2-}	$H_2PO_4^-$	Average
Optical mass (ng/cm^2)[a] [A]	2540	2270	2230	2230	2318 (±150)
Wet mass (ng/cm^2)[b] [B]	5350	3750	3830	5230	4540(±870)
Water content (%) [100×((B-A)/B)]	53	39	42	57	48 (±9)
Frequency shift upon salt exposure ($\Delta f_3/3$, Hz)	-2.04	2.58	-5.77	-18.54	-

a) As-prepared in 0.15 M NaCl, before the exposure to the sodium salt solutions. Dry mass calculated by the model-based optical thickness, assuming a PEM density of 1 g/cm^3.
b) As-prepared in 0.15 M NaCl, before the exposure to the sodium salt solutions, obtained via the Sauerbrey equation.

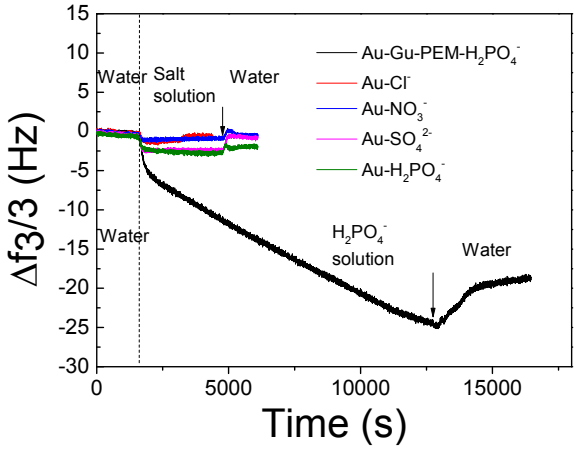

Fig. S4. The frequency shifts at the third harmonic ($\Delta f_3/3$) as a function of time, recorded for bare QCM sensors exposed to different anion solutions containing 10 mM Cl^- (red line), NO_3^- (blue line), SO_4^{2-} (pink line), and $H_2PO_4^-$ (green line), respectively. The frequency shift for the PAH-containing PEMs exposed to the $H_2PO_4^-$ solution (black line) is also presented. The dashed line indicate the moment in time at which the salt solutions were exposed to the QCM sensors; the arrows indicate the moment at which the solution was replaced by Milli-Q water again.

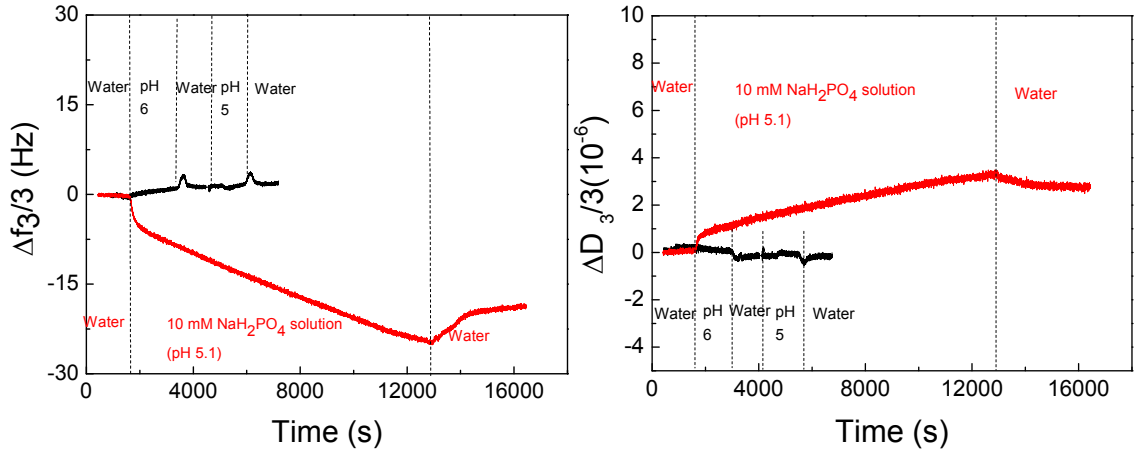

Fig. S5. The frequency and dissipation responses for a QCM sensor modified with a PAH-Gu PEM when i) exposed to the solutions with pH 6 and 5 (black curve), and ii) exposed to 10 mM NaH_2PO_4 at pH = 5.1 (red curve). The dashed lines indicates the moments in time at which the solution conditions were changed.

Table S3. The frequency response, areal mass of PEMs and the density of ions in the multilayers calculated using the Sauerbrey equation.

Ion	M_w (g/mol)	ΔM_w (g/mol) w.r.t. Cl^-	$\Delta f_3/3$ (Hz)		Mass (ng/cm^2)		Density (anions/nm^2)	
			PAH/ PSS	PSS/ PAH-Gu	PAH/ PSS	PSS/ PAH-Gu	PAH/ PSS	PSS/ PAH-Gu
Na^+	23	-	-	-	-	-	-	-
Cl^-	35.5	0	-0.84	-2.04	15.01	36.43	-	-
NO_3^-	62	26.5	0.11	2.58	-2.00	-46.2	-	-
SO_4^{2-}	96	60.5	-0.28	-5.77	4.99	103.33	0.08	1.71
$H_2PO_4^-$	97	61.5	-3.50	-18.54	62.60	331.81	1.02	5.39

Table S4. Molecular weights, crystal radii, hydrated radii, and hydration energies of several ions.

Ion	M_w (g mol^{-1})	Crystal radius[a] (nm)	Hydrated radius[b] (nm)	$\Delta G_{hydration}$[a] (kJ mol^{-1})
Cl^-	35.5	0.181	0.195	-340
NO_3^-	62.0	0.179	0.340[c]	-300
SO_4^{2-}	96.0	0.230	0.300	-1080
$H_2PO_4^-$	96.0	0.200	0.302	-465
PO_4^{3-}	95.0	0.238	0.339	-2765
Na^+	23	0.102	0.178	-365

a) Ref 4, b) Ref 5, c) Ref 6.

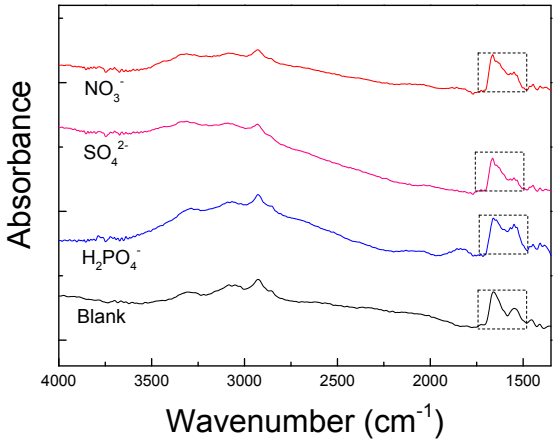

Fig. S6. RAIR spectra of PSS/PAH-Gu multilayers before and after exposure to aqueous solutions of NaH_2PO_4, Na_2SO_4 and $NaNO_3$.

To study the effect of NaH_2PO_4, $NaNO_3$ and Na_2SO_4 exposure onto the characteristic IR peaks of PAH-Gu, the PEM-modified sensor surfaces were characterized by RAIR. The N-H bands in the region of 3200 to 3600 cm^{-1} present in the spectra of PSS/PAH-Gu PEMs did not shift upon the exposure to the aqueous salt solutions (Fig. S6 and Table S5). However, some changes were observed in the range from 1800 to 1400 cm^{-1}. The two strongest absorption bands peaks present in this region are associated to the amide groups and guanidinium groups as shown in the blank PSS/PAH-Gu PEM (Fig. S7a). When exposed to the different sodium salts, the characteristics in this region were found to change mostly for multilayers exposed to NaH_2PO_4 (Fig. S7b-d). This can be rationalized by comparing the IR spectra of the salts, from which it becomes clear that only NaH_2PO_4 shows a strong absorption band in the range from 1500 to 1700 cm^{-1} (Fig. S8).

Table S5. Characteristic infrared bands of RAIR spectra (Fig. S6) of PSS/PAH-Gu multilayers after exposure to aqueous solutions of NaH_2PO_4, $NaNO_3$, and Na_2SO_4 (wavenumbers in cm^{-1}).

System	ν (N-H)	ν (C=N, guanidino) and ν_a (C=O, amide) (bands overlapped)	ν_s (C-N, N-H bending, amide)	Normalized Integrated Area (1750-1500 cm^{-1})
PEM (no salt)	3304	1661	1547	1
PEM/$H_2PO_4^-$	3294	1661	1548	1.35
PEM/SO_4^{2-}	3309	1664	1549	1.05
PEM/NO_3^-	3309	1663	1549	0.83

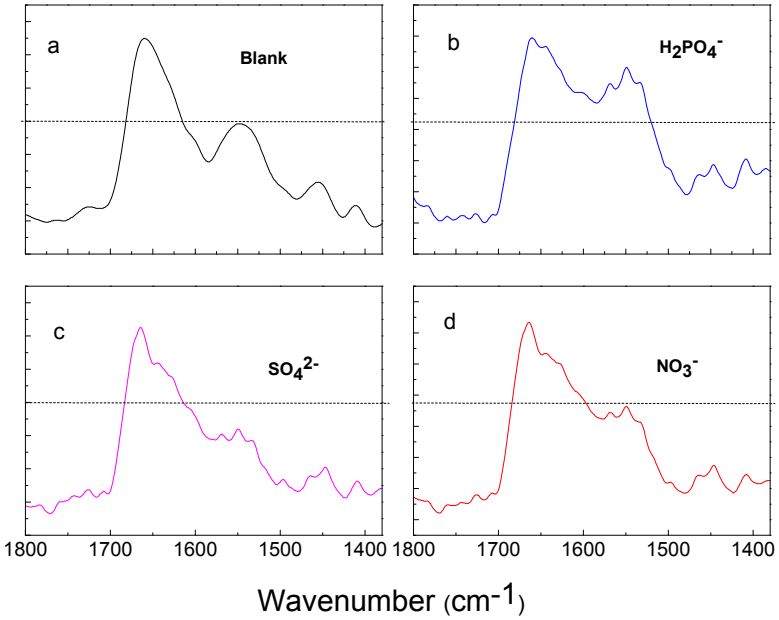

Fig. S7. Region (1380-1800 cm^{-1}) Reflection Absorption IR spectra of a PSS/PAH-Gu PEM on a gold (QCM) surface, a) before and after the exposure to aqueous solutions of b) $H_2PO_4^-$, c) SO_4^{2-} and d) NO_3^-.

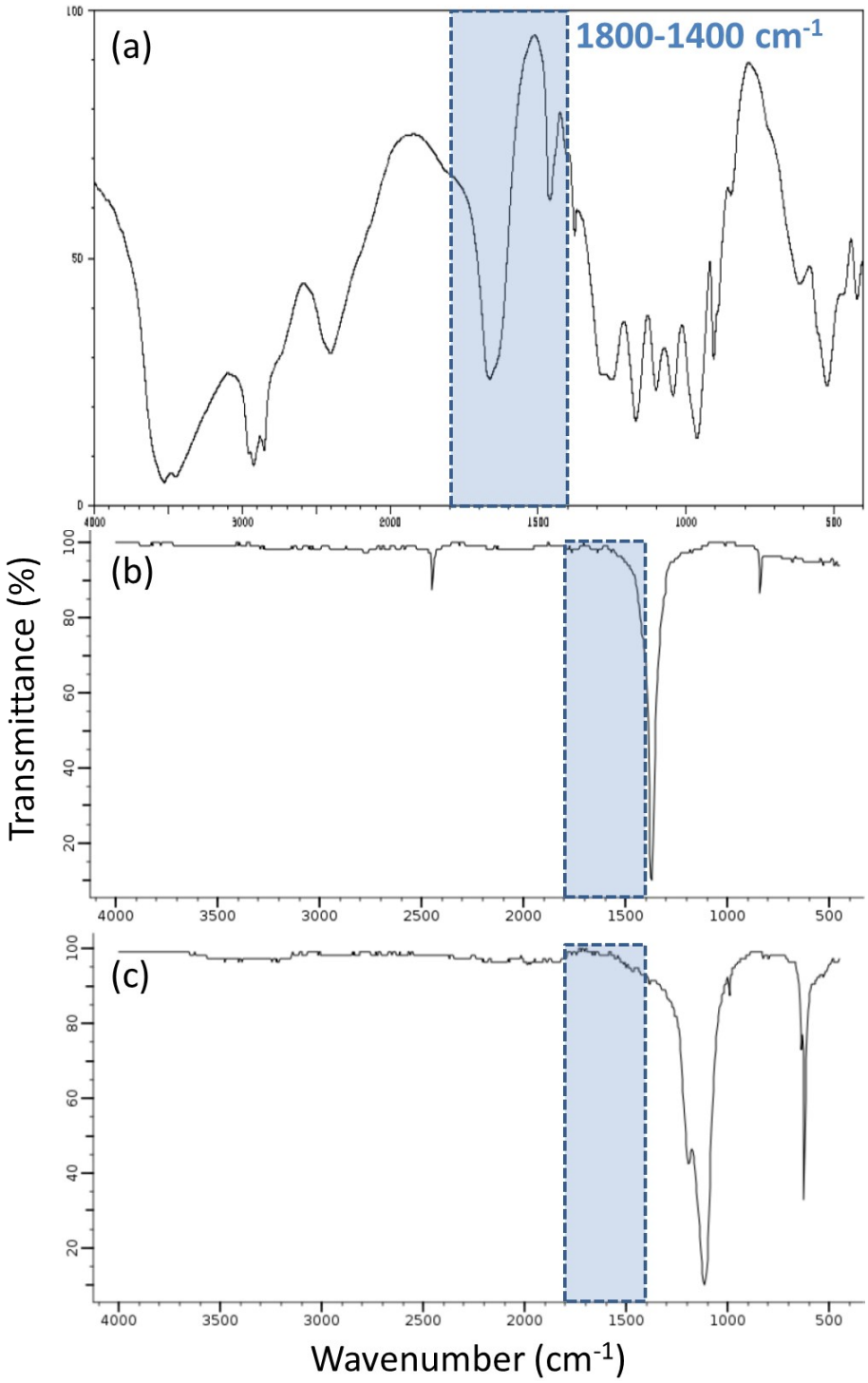

Fig. S8. Reference FT-IR spectra of a) NaH_2PO_4, b) Na_2SO_4 (b), and c) $NaNO_3$ (c). Spectra obtained from http://www.cas.org/products/scifinder in September 2014. The indicated areas cover the region of 1800 to 1400 cm^{-1}.

References

1. N. M. Alves, C. Picart and J. F. Mano, *Macromol. Biosci.*, 2009, **9**, 776.
2. F. Höök, B. Kasemo, T. Nylander, C. Fant, K. Sott and H. Elwing, *Anal. Chem.*, 2001, **73**, 5796.
3. S. M. Notley, M. Eriksson and L. Wågberg, *J. Colloid Interface. Sci.*, 2005, **292**, 29.
4. J. W. Steed and J. L. Atwood, *Supramolecular Chemistry*, 2nd ed. John Wiley & Sons, Ltd, Chichester, UK, 2009, p. 226.
5. M.Y. Kiriukhin and K.D. Collins*, Biophys. Chem.*, 2002, **99**, 155.
6. B. Tansel, J. Sager, T. Rector, J. Garland, R. F. Strayer, L. Levine, M. Roberts, M. Hummerick, J. Bauer, *Sep. Purif. Technol.*, 2006, **51**, 40.